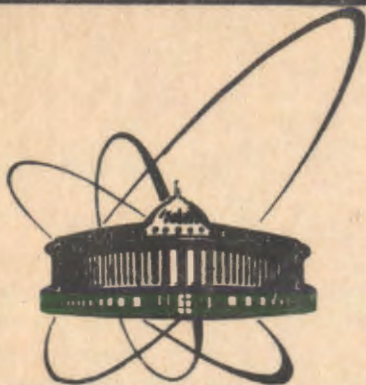


90-593



сообщения
объединенного
института
ядерных
исследований
Дубна

E13-90-593

L. M. Soroko

LONGITUDINAL INTERFERENCÉ
OF THE DIFFRACTION FREE WAVE FIELDS.
II. EXPERIMENTS

1990

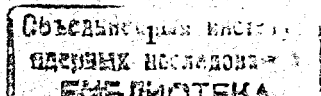
I. INTRODUCTION

In the previous paper^{/1/} the new phenomenon, "the longitudinal interference of the diffraction free wave fields", was introduced and explained, and the experimental arrangements designed for observation of the longitudinal interference were described: the system with two coaxial circular diffraction gratings, the system with two narrow coaxial transmitting rings and the system with one circular diffraction grating which generates at least two diffraction orders. The evolution of the structure of the longitudinal interference of the light in the volume between the generator and the detector was analysed. Finally the technique for suppressing the longitudinal modulation of the light intensity on the optical axis of the system with two coaxial conical wave fronts has been suggested.

In this paper the experiments with narrow coaxial transmitting rings on the screen are described in detail. The measurements of the longitudinal modulation of the light intensity on the optical axis of the system are presented. The structures of the wave field at various evolution stages of the longitudinal interference in the volume between the generator and the detector are demonstrated. Then the experiments with straight line 180° phase jump on the optical plate in the system with two coaxial conical wave fronts are described.

2. EXPERIMENTS WITH TWO NARROW COAXIAL TRANSMITTING RINGS

Among the possible experiments suggested for observation of the longitudinal interference of the light^{/1/} the technique with two narrow coaxial transmitting rings was chosen as the most accessible one. The experimental arrangement is shown in Fig.1. The collimated beam of light from laser I is transformed by the objective lens 2 into the convergent beam of light which goes through the pinhole in the screen 3. The second objective lens 4 produces the single mode beam of light which illuminates the screen 5 with narrow coaxial transmitting rings. The screen 6 restricts the number of the narrow coaxial



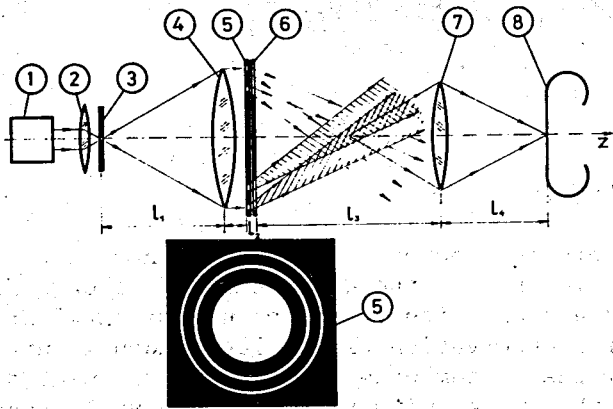


Fig. 1. The experimental arrangement used for observation of the longitudinal interference of the conical wave fronts which were generated by narrow coaxial transmitting rings: 1 - laser, 2 - objective lens, 3 - the screen with pinhole, 4 - the second objective lens, 5 - the screen with narrow coaxial transmitting rings, 6 - the cut-off screen, 7 - the imaging objective lens, 8 - photofilm.

transmitting rings which contribute to the interference picture. Each narrow transmitting ring of the width $20 \mu\text{m}$ on the screen 5 was fabricated by the laser photosynthesizer^{1,2,3/}. The diameter of the focused laser spot was equal to $1 \mu\text{m}$. The groves on the glass backing produced in such a device are working as a circular diffraction grating, and the observer sees the rainbow spectra on placing the screen 5 between the glow lamp and the eye.

The system of 10 narrow coaxial transmitting rings with spacing $200 \mu\text{m}$ was fabricated by the technique^{3/} for the simulation experiments of the direct search of the "stars" in the nuclear emulsion by means of the kinoform with ring response^{4/}.

The components of the diffracted light from each transmitting ring are going initially separately, then they are mutually crossing near the optical axis of the system. The objective 7 produces the image of the interference picture in one of the plane which is perpendicular to the optical axis of the system on the photofilm 8. Various parts of the volume between the generator and the detector in which we observe the structure of the wave field at various evolution stages of the longitudinal interference are shown in Fig. 2. In the plane A we see the narrow coaxial transmitting rings in focus of the objective 7. In the plane B some kind of self-imaging of the Talbot type^{5,6/} can be observed. In the plane C only partial overlap-

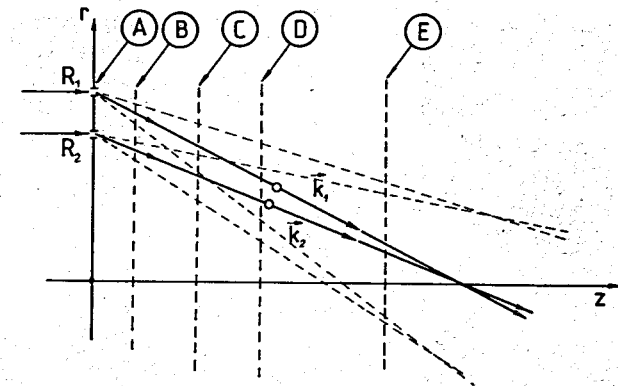


Fig. 2. Different parts of the volume between the screens 5 and 6 (generator) and the observation plate (detector) in which the interference picture has different structure: R_1 and R_2 - two narrow coaxial transmitting rings, k_1 and k_2 - the wave vectors which define the corresponding conical (quasi conical) wave fronts.

ping of the light components going from adjacent coaxial rings is taking place. In the region D we see the complete overlapping of these components but at some distance from the optical axis of the system. Only in the region E the interference picture approaches the optical axis of the system from all azimuthal directions.

The photo of the fragment of two coaxial transmitting rings in the plane A is shown in Fig. 3. The interference picture in the plane C is presented in Fig. 4. The corresponding picture in the region D is given in Fig. 5. The interference fringes in the region E in the vicinity of the optical axis of the system are shown in Fig. 6.

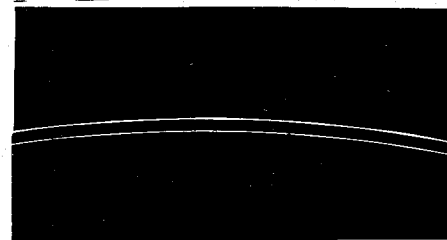


Fig. 3. The fragment of two rings in the plane A.

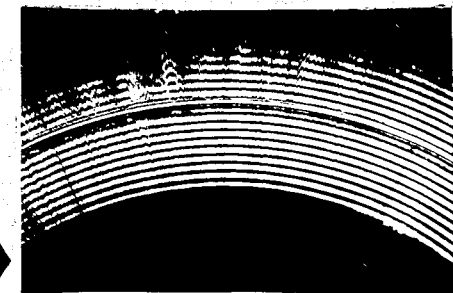


Fig. 4. The structure of the interference picture in the plane C.

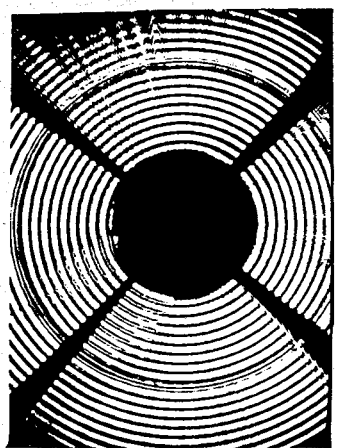


Fig. 5. The structure of the interference picture in the region D.

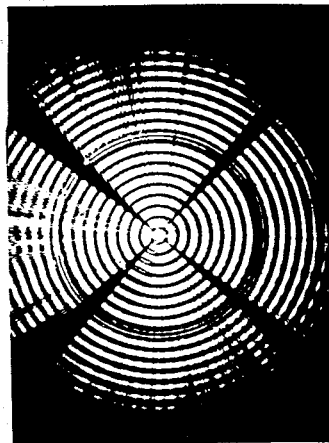


Fig. 6. The structure of the interference picture in the region E.

The positioning of the maxima and minima of the longitudinal modulation of the light intensity on the optical axis of the system is given in Fig. 7. As the angle between two wave vectors \vec{k}_1 and \vec{k}_2 is very small, $\sim 10^{-4}$ radian, the period A of this modulation is of the order of 10 mm. There were estimated 12 maxima and minima on the optical axis. From Fig. 7 we may conclude that the period A is a slow varying function of z -coordinate. This is a natural consequence of the fact that each

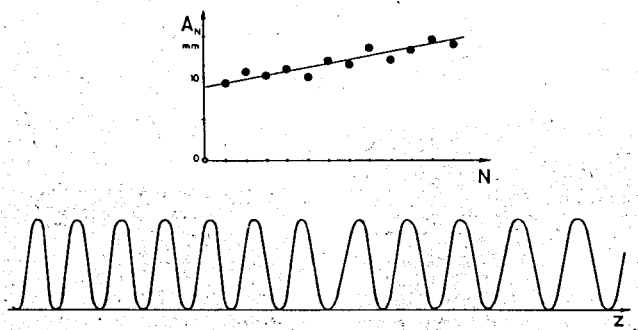


Fig. 7. The distribution of the light intensity on the optical axis and the dependence of the period A versus the number N of the maximum.

narrow transmitting ring contributes to the interference picture as a point-like source of light and due to this the angle between the wave vectors \vec{k}_1 and \vec{k}_2 is varying inversely proportional to the distance from the screen 5 to the observation point.

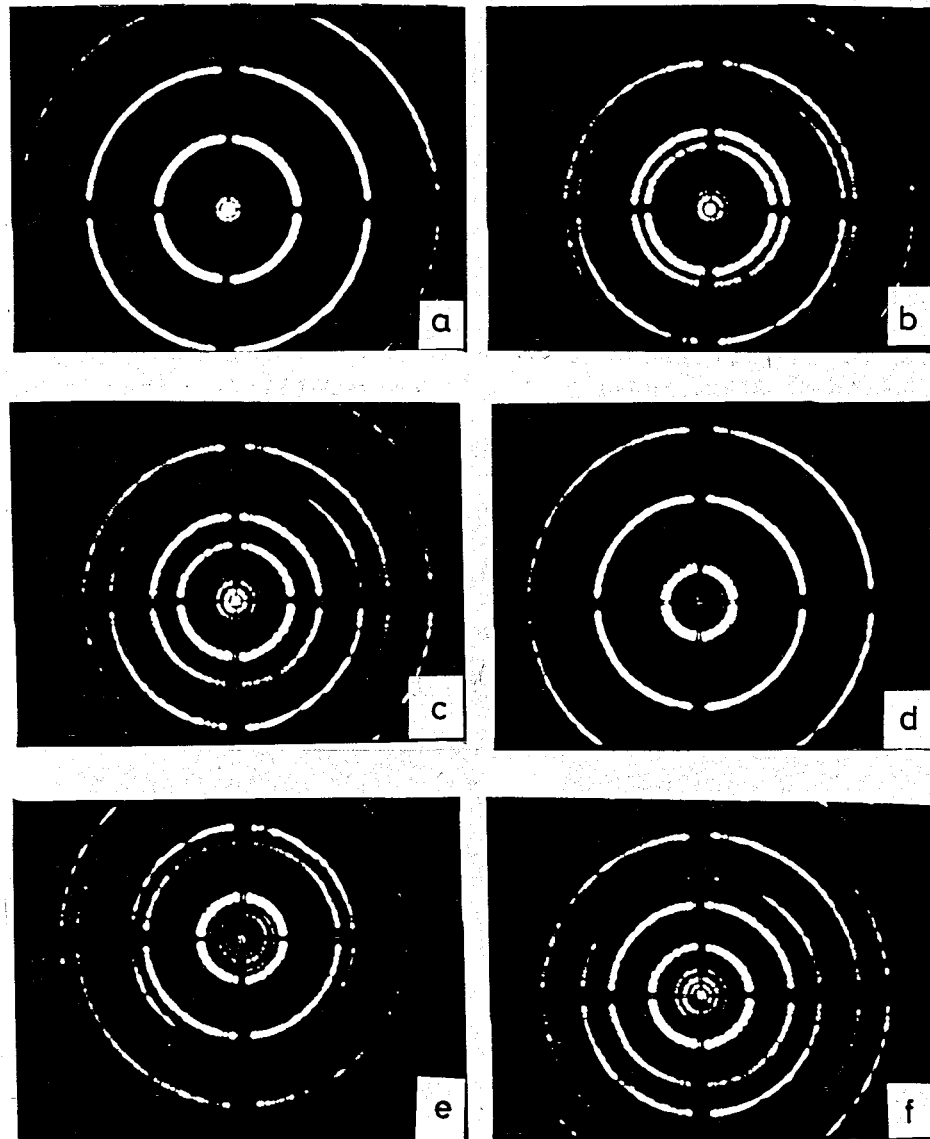


Fig. 8. The evolution of the interference picture along z -axis of the system: a, b, c, d, e, f (see text).

The longitudinal interference of the light in the vicinity of the optical axis is the result of the mutual superposition of two interference pictures going from two opposite directions. Each contributing picture moves to the optical axis, then crosses it and finally goes away from the optical axis. To show this process on the photons we chose the experimental arrangement in which the number of the narrow coaxial transmitting rings is equal to 10. In this condition the width of the main maxima of the interference pictures was small with respect to the period A of the intensity light modulation, and we can observe the mentioned dynamics of the mutual superposition of two contributing pictures.

The picture shown in Fig.8a was taken in the position where two contributing interference components going in the opposite directions coincide mutually, and the light intensity on the optical axis is maximal. The picture given in Fig.8b was taken at z -coordinate where those two contributing interference components are separated and are seen in the form of the doublet. At the next stage shown in Fig.8c the separation between the components of this doublet is larger than in Fig.8b. At the position presented in Fig.8d these two contributing interference components are in the antiphase in such a manner that the total intensity of the light on the optical axis is minimal (zero). At the next stage these components are separated again (Fig.8e). Finally we present the photo taken in the position when the intensity of the light on the optical axis is maximal though the contributing interference components do not coincide in this plane (Fig.8f).

3. EXPERIMENTS WITH STRAIGHT LINE 180° PHASE JUMP PLATE

To demonstrate the feasibility of the technique suggested in¹¹ with the purpose to suppress the longitudinal modulation of the light on the optical axis of the system with two coaxial narrow transmitting rings we have accomplished the simulation experiments with straight line 180° phase jump on the optical plate^{7,8} for He-Ne laser. On Fig.9 we see general positioning of this straight line 180° phase jump and the system of two coaxial narrow transmitting rings. The straight line of the 180° phase jump must cross at least one of two coaxial rings. In Fig.10 one of such arrangement is shown. The photo of this arrangement in the plane A is presented in Fig.11. The points of zero intensity are marked by the white

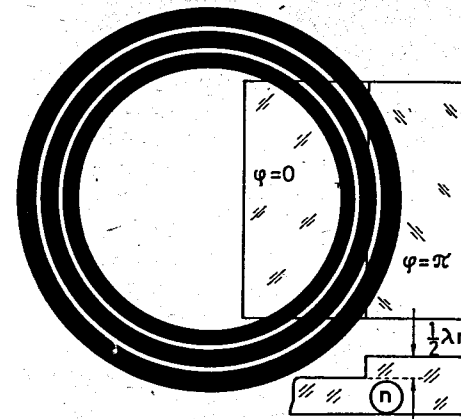


Fig.10. The arrangement of the straight line 180° phase jump in the experiment when the straight line crosses only one (external) ring.

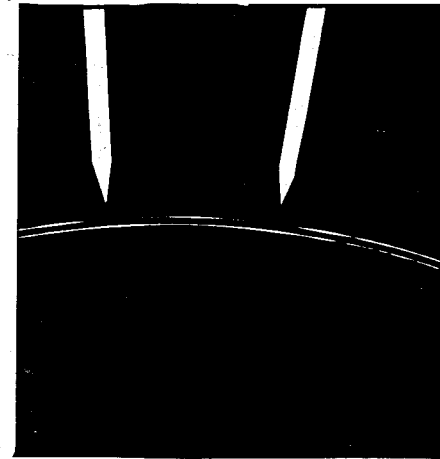


Fig.12. The structure of the interference picture in the experimental condition presented in Fig.10 in the region D.

Fig.9. The view of the straight line, 180° phase jump and of the rings.

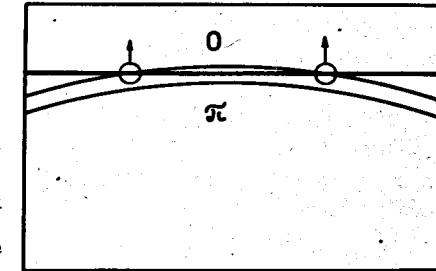
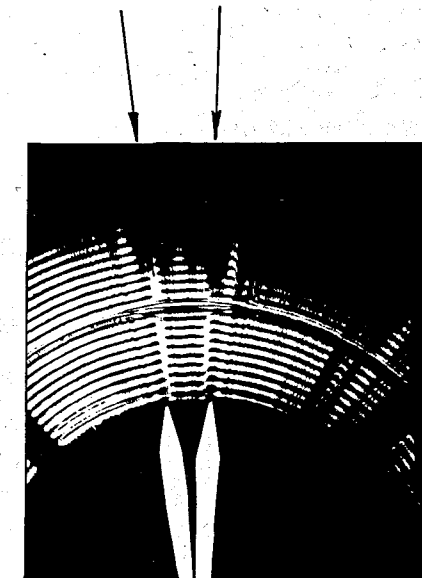


Fig.11. The photo of the arrangement shown in Fig.10 in the plane A.



arrows. The structure of the interference picture in the plane D is given in Fig.12. The radial lines where we see the phase jumping of the interference picture are marked by the white and black arrows. These phase jumping correspond to the points where antiphasing of the interference pictures are taking place. The dark ring arc at constant distance to the optical axis goes into the bright ring arc and vice versa, the bright ring arc goes into the dark ring arc. The interference picture taken in the position when it reaches the optical axis is shown in Fig.13. As the length of the phase jumped arc is small with respect to the length of the circle these local phase jumpings cannot change the distribution of the light intensity on the optical axis of the system.

In the second experiment the straight line phase jump crosses two coaxial transmitting rings (Fig.14). The photo of this arrangement in the plane A is given in Fig.15. Now two points of zero intensity marked by the white arrows in Fig.15 are on both rings. The structure of the interference picture in the region D is presented in Fig.16. Four radial lines on which the phase jumpings are taking place are marked by the black arrows. We see that the central part of the ring arc at constant distance to the optical axis is in the phase with external parts of this ring arc.

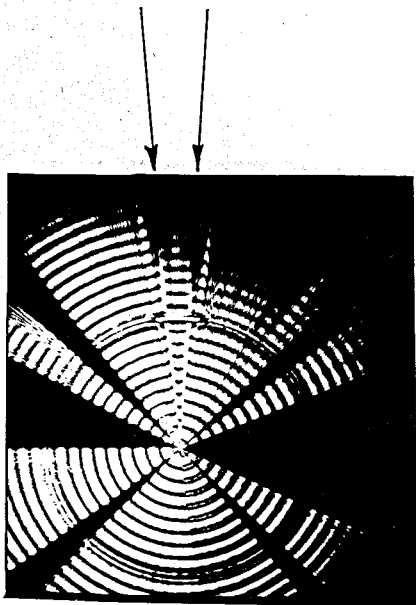


Fig.13. The structure of the interference picture in the experimental condition presented in Fig.10 in the region E.

Fig.14. The arrangement of the straight line 180° phase jump in the second experiment when the straight line crosses both external and internal rings.

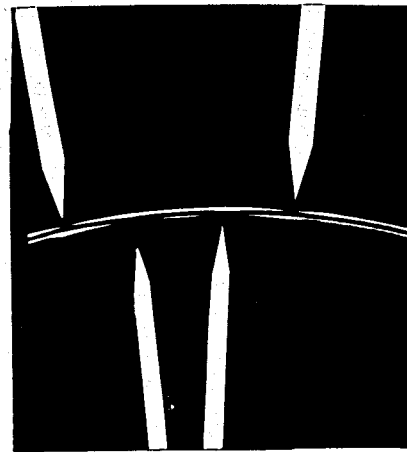
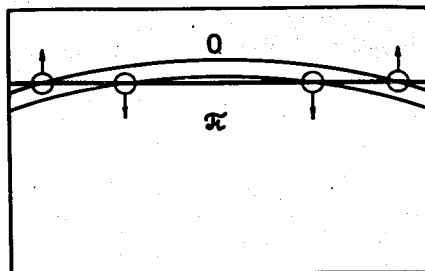
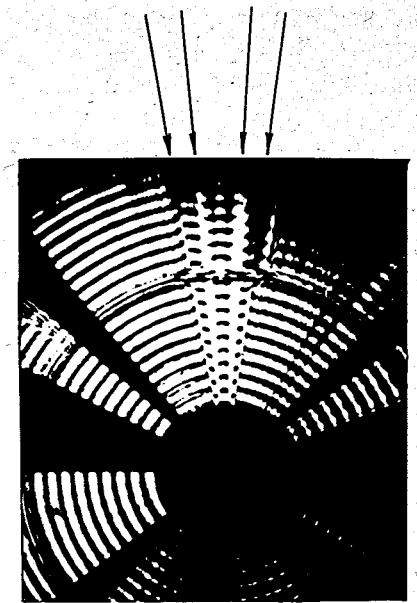


Fig.15. The photo of the arrangement shown in Fig.14 in the plane A.

Fig.16. The structure of the interference picture in the condition of the second experiment shown in Fig.14 in the region D.



4. EXPERIMENTS WITH MANY NARROW COAXIAL TRANSMITTING RINGS

If the number of the narrow coaxial transmitting rings is more than two the interference fringes have more complicated structure. To estimate the main features of this complex interference picture we consider two cases: a) 4 rings and b) 10 rings. The photos of these rings in the plane A are shown in Figs. 17 and 18. The dark gap in the central part of

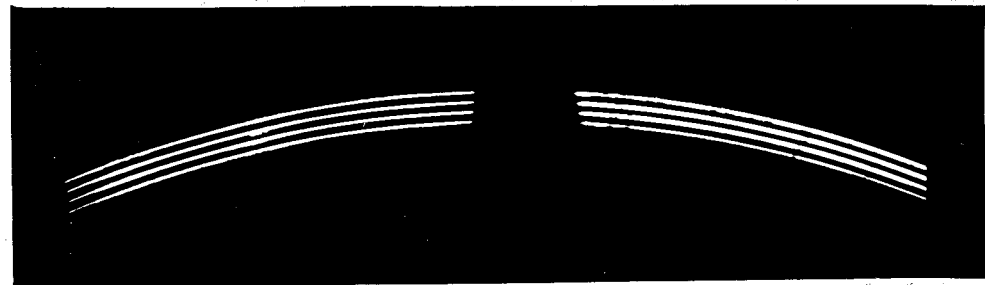


Fig.17. The photo of 4 narrow coaxial transmitting rings in the plane A.

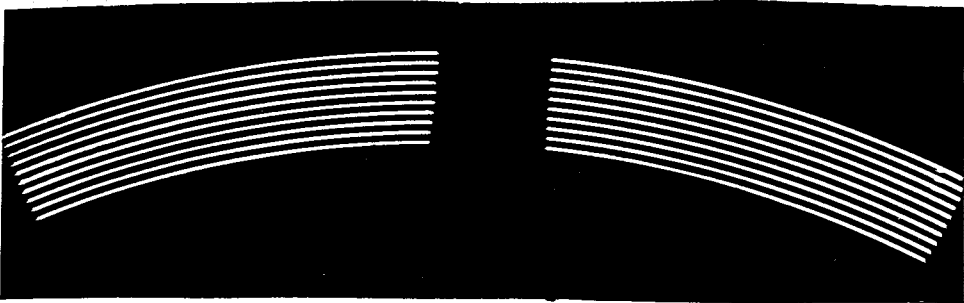


Fig.18. The photo of 10 narrow coaxial transmitting rings in the plane A.

the photo is the shadow from one of four supporting strips of the black paper screen 6. The interference picture in the region E for the case of four rings given in Fig.19 consists of three intermediate minima and two secondary maxima. This feature follows from the theorem presented in¹¹: the function $a(z)$ which describes the amplitude of the longitudinal interference of many coaxial conical wavefronts is equal to the Fourier Transform of the angular field $g(\theta)$ of the contributing wave vectors.

The most pronounced phenomena can be observed in the case of 10 rings. The photo of these rings in the plane A was shown in Fig.18. In the region B we see self-imaging Talbot effect^{5,6} presented for one definite plane in Fig.20. The interference picture for 10 rings in the region D is given in Fig.21. This picture consists of one main maxima and many secondary maxima and minima.

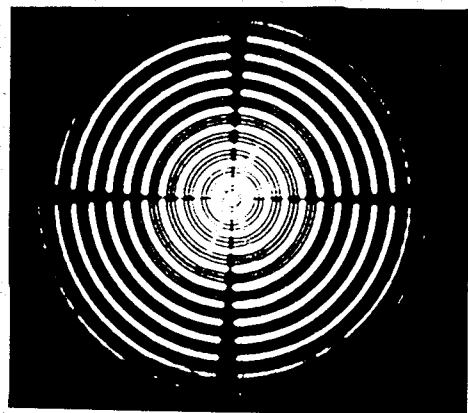


Fig.19 The structure of the interference picture observed in the region E in the case of 4 rings.

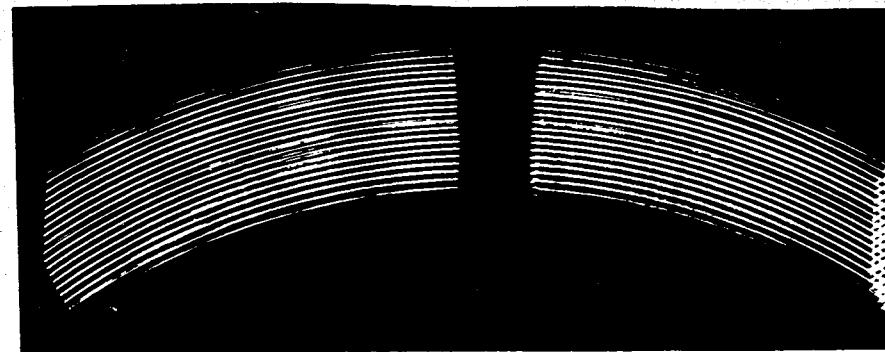


Fig.20. The self-imaging Talbot effect in the case of 10 rings.

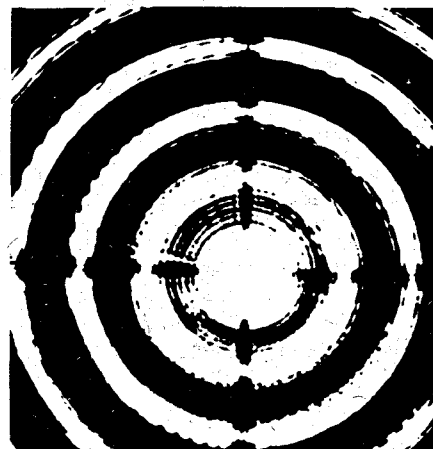


Fig.21. The structure of the interference picture in the region E in the case of 10 rings.

REFERENCES

1. Soroko L.M. - Communication of the JINR, E13-90-592, Dubna, 1990.
2. Koronkevich V.P. et al.- *Optik*, 1984, 67, 257.
3. Koronkevich V.P. et al.- Preprint of the Institute of Automation and Electrometry, Sib. Br. Ac. Sci. USSR, No.421, 1989.
4. Bencze G.L. et al. - Communication of the JINR, P13-87-474, Dubna, 1987.
5. Talbot F. - *Lond. Edinb. Dubl. Phil. Mag.*, 1836, 9, 401.
6. Denisyuk Yu.N. et al. - *Optika i spektroskopiya*, 1971, 30, 1130.

7. Lowenthal S., Belvaux Y. - Appl. Phys. Lett., 1967, 11, 49.
8. Soroko L.M. - Hilbert-Optics, Nauka, Moscow, 1981.

Received by Publishing Department
on December 28, 1990.